Advance Physics Letter

Removal of toxic Cd^{+2} ions using nano magnetite loaded Alginate/PVA hydrogel spheres in fixed bed column from aqueous solution

[1]Prerna Kathane & [2]Alka Tiwari

[1,2]Department of Chemistry, Government Vishwanath Yadav Tamskar Post Graduate Autonomous College, Durg (Chhattisgarh) 491001, INDIA
Email: [1]prernakathane04@gmail.com & [2]alkatiwari18 @gmail.com

Abstract: Effective removal of toxic Cd(II) ions from aqueous solution using nano magnetite loaded polyvinyl alcohol-alginate hydrogel spheres (PVA-ANM) has been explored by column adsorption system. Co-polymer was magnetized in-situ and characterized by TEM, SEM, XRD, FTIR and VSM analysis. Effect of bed height, feed flow-rate and inlet Cd^{2+} ions concentration on breakthrough characteristics of sorption were examined in fixed-bed column. The Thomas, Yoon-Nelson and BDST empirical models are fitted well with the data obtained by experiments and constants were evaluated. Suitability of adsorbent tested with the Cd ions containing water samples collected from various field. This adsorbent revealed ≥ 98 % removal of Cd^{2+} ions and could be regenerated efficiently and reused.

Keywords: Cd(II) ions, nano magnetite, fixed-bed column, adsorption kinetics, polyvinyl alcohol-alginate

I. INTRODUCTION

Water contamination by heavy metals such as As, Cd, Cu, Cr, Fe, Pb, Hg, Ni and Zn are serious environmental concern globally[1, 2]. However, Cd^{2+}, Zn^{2+}, Fe^{2+} ions are essential micro-nutrients for living organisms, but when it present in excess, they can become extremely toxic. These metals are not biodegradable and tend to accumulate in living organisms causing diseases and disorders in its functioning. Cadmium is listed as one of the 126 priority toxicants by USEPA and as a known carcinogen by International Agency for Research on Cancer. Science Asia 2004 also quoted that Cd(II) pollution has induced extremely adverse effects on plants and animals. Chronic dust or fume exposure can give permanently damage to the lungs, producing shortness of breath and emphysema [4, 5]. The maximum allowable limit for Cd^{2+} ions concentration set 0.01 mg/L by the WHO [6]. Industries like electroplating, Ni–Cd batteries, pigments, plastics, pesticides, dyes, textile and mining, waste water contain undesired amounts of Cd^{2+} ions.

Cadmium poisoning may be acute by ingestion/ inhalation, in chronic exposure and it accumulates in body, particularly the kidney and liver, causing kidney damage, renal disorder, bone fracture, high blood pressure, destruction of RBC, diarrhea, infertility, psychological disorders, damage to central nervous system, immune system, cancer and muscle cramps etc. Hence it becomes necessary to remove toxic Cd(II) ions from municipal and industrial effluents to protect plants, animals and human beings from their adverse effects before discharging into natural water bodies [4,7].

Adsorption is one of promising removal process which extensively applied in the field of water remediation among numerous reported methods like filtration, solvent extraction, ion-exchange, membrane-process, electrolysis etc [8–14]. Several adsorbents including agricultural waste, industrial by-products natural and synthetic polymers [15-23] activated carbon, metal hydroxide, hydrogel, nano magnetite loaded synthetic hydrogel etc have been applied for Cd(II) ions removal [24-29]. Unfortunately most of these adsorbent have drawbacks like high capital and operation cost, disposal of sludge and are inadequate when allowable concentrations of metal ions are very low. Hence systematic treatment strategies which are simple, consistent and involving local resources of Cd(II) ions removal from wastewater necessitate for substantial environmental significance.

In present research work a novel adsorbent polyvinyl alcohol and alginate bound nano magnetite hydrogel spheres (PVA-ANM) have been reported for Cd^{+2} ions uptake from water. The blend technique sorption and magnetic separation involved in removal process. Regeneration of adsorbent and recovery of metal ions are very advantageous and provoking.

II. EXPERIMENTAL

2.1 Materials:- The $Cd(NO_3)_2\ 4H_2O$, sodium alginate, polyvinyl alcohol, NaOH pellets were purchased from Loba Chemie Mumbai, India. $FeCl_2\ 4H_2O$, anhydrous $FeCl_3$ and HCl were purchased from Molychem, Mumbai, India. Triple distilled water was used throughout the experiments.

2.2 Synthesis of PVA-ANM microspheres

The adsorbent were prepared in four steps:-

The first step involves the preparation of viscous gel of polyvinyl alcohol (PVA) by dissolving at 90°C in hot triple distilled water and was mixed thoroughly with the sodium alginate to get 1:1 ratio, stirred for an hour for homogeneity and kept aside to obtain a bubble free solution.

In second step the hydrogel spheres were prepared by drop wise addition of the above mixture in $CaCl_2$ solution (0.5M) for cross linking. The hydrogel spheres so produced were allowed to harden by leaving them in solution for 24h then filtered and washed several times with distilled water.

In the third step, these hydrogel spheres were equilibrated in an aqueous solution of ferrous chloride tetrahydrate and ferric chloride in 1:3ratio for 24h.

In fourth step for insitu magnetization these iron-oxide loaded hydrogel spheres were added into alkaline solution and kept for 2 h, so that Fe^{2+}/Fe^{3+} ions get precipitated into nano iron-oxide within PVA-Alginate matrix. These PVA-ANM hydrogel spheres were then thoroughly washed several times and stored for studies.

2.3 Preparation of Stock Solution:- Stock solution of Cd (II) was prepared by dissolving 2.640 g of Cd $(NO_3)_2.4H_2O$ in 1000 mL distilled water. Working standards was freshly prepared by appropriate dilution of stock in each experiment. Triple distilled water was used throughout experiment.

2.4 Characterization:- Adsorbent PVA-ANM was characterized by XRD, FTIR, SEM, TEM and VSM analysis

2.5 Column Adsorption Study:- Fixed-bed adsorption experiments were performed in a Pyrex glass column (1 cm diameter and 15 cm height) at pH 4 and temperature 25(±2) ℃. Column was packed with various bed heights of PVA-ANM adsorbent on a glass-wool support. A known concentration of Cd^{+2} ions solutions was allowed to pass through bed at a constant flow-rate 1 mL/min in a continuous down flow manner.

The Cd solution was then collected at various time intervals until the column reached exhaustion. Concentration of Cd (II) ions was assessed by AAS (Atomic Adsorption Spectrophotometer).

2.6 Analysis of Column Parameters:- The efficiency and nature of Cd^{2+} ions adsorption was calculated by the breakthrough curves of fixed-bed column. The maximum removal capability q_{total} for a given flow rate and inlet Cd^{+2} ions concentration is determined by Eq. 1.

$$q_{total} = \frac{QA}{1000} = \frac{Q}{1000} \quad (1)$$

where q_{total} , Q and A are the total flow time (min), flow-rate (mL/min) and area under breakthrough curve, respectively. The Cd^{+2} ions removal capacity q_{eq} (mg/g) is defined as q_{total} per g of sorbent (m) at the end of total flow time is evaluated by Eq. 2

$$q_{eq} = \frac{q_{total}}{m} \quad (2)$$

The total amount of adsorbate passed through column (m_{total}) and maximum % removal are evaluated by Eq. 3 and 4

$$m_{total} = \frac{C_i Q t_{total}}{1000} \quad (3)$$

$$\% \text{ Removal} = \frac{q_{total}}{m_{total}} \times 100 \quad (4)$$

2.7 Modeling Dynamics of Column

The adsorption performance of Cd(II) ions onto PVA-ANM bed was examined by Thomas, Yoon-Nelson and BDST empirical models using Eq. 5, 6 and 7, respectively.

$$\ln\left(\frac{C_i}{C_t} - 1\right) = \frac{K_T q_o M}{Q} - \frac{K_T C_I}{Q} V \quad (5)$$

where C_t and C_i is effluent and influent solute concentration (mg/L) respectively, Q is flow-rate (mL/min), q_o is adsorption capacity (mg/g) K_T is Thomas rate constant(mL/min. mg) and V is through put volume (mL).

$$\ln\frac{C_t}{C_i - C_t} = K_{YN}\, t - \tau . K_{YN} \quad (6)$$

where K_{YT} (L/min) is Yoon-Nelson rate constant, τ is time required for 50% adsorbate breakthrough (min) and t is sampling time.

$$t = \frac{N_0}{C_i} Z - \frac{1}{K_a C_i} \ln\left(\frac{C_i}{C_t} - 1\right) \quad (7)$$

where K_a is rate constant (L/mg. min) and N_0 is column capacity (mg/L)

2.8 Column Desorption Study

Column desorption was examined by using 0.1M HCl solution at temperature 25℃ with flow-rate 1 mL/min and 10 cm bed height for 360 min. The regenerated columns were reactivated by washing bed thoroughly with hot distilled water and may be reused for further experiments.

III. RESULTS AND DISCUSSION

3.1 Characterization of PVA-ANM

SEM Analysis:-Scanning electron microscopy (SEM) images of (a) bare & (b) Cd(II) ions adsorbed PVA-ANM are depicted in Fig-1 heterogeneous surface has porous type of physiology; clusters of iron-oxide with vitiate ranging in width to as large as 50 μ m. Morphology and surface texture definitely accounts for the valuable adsorbing property of adsorbent [30].

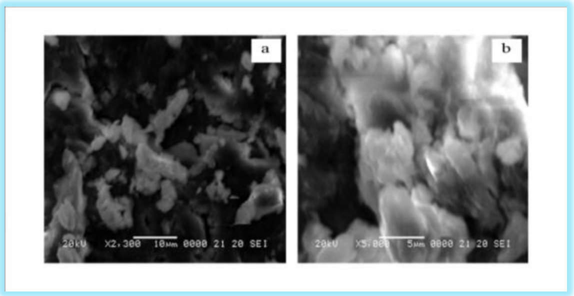

Fig: 1 SEM Images of PVA-ANM

FT-IR Analysis:-By comparing FT-IR vibrancy signals of PVA-ANM of (a) bare and (b) Cd(II) loaded (Fig 2). Following conclusions could be drawn; Slight shifting of –OH stretching band from 3416 to 3409 cm^{-1} suggests the attachment of adsorbate Cd^{2+} ions, shifting of C=O asymmetrical stretching band from 1420 to 1415 cm^{-1} is due to the association of Cd (II) ions on -COO group. Shifting of C-O band to the lower frequency from 1032 to 1025 cm^{-1} can be attributed to association of adsorbate. Slight shift of Fe-O band from 529 to 518cm^{-1} shows uptake of some Cd(II) ions on nano iron-oxide surface.

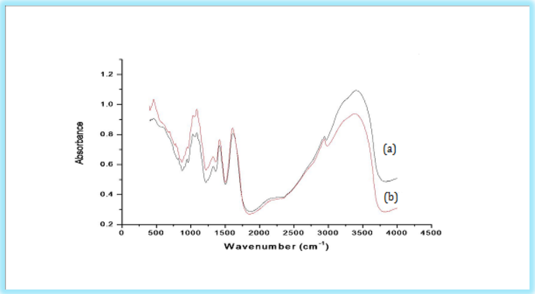

Fig: 2 FT-IR Pattern PVA-ANM

XRD Analysis:-The XRD pattern of PVA-ANM (Fig 3) exhibited five characteristics peaks (2θ = 26.93, 31.89, 38.87, 41.23 and 45.55). Position and relative intensities of all diffraction peaks in match well with JCPDS file No. 89-5984 for magnetite (Fe_30_4) and reveal that prominent phase formed is nano magnetite Fe_30_4 with cubic structure, 36.93nm crystallite size by following reaction:-

$$2FeCl_3 + FeCl_2 + 8NH_4OH \rightarrow Fe_3O_4 + 8NH_4Cl + H_20$$

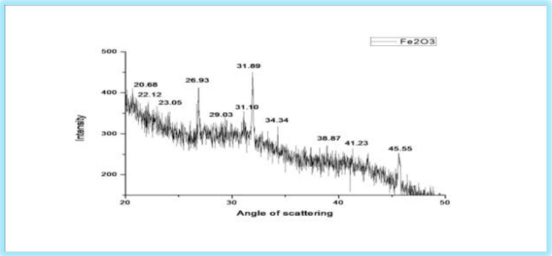

Fig: 3 XRD Pattern of PVA-ANM

VSM Analysis: Vibrating Sample Magnetometer followed Longevin function with co-reactivity and zero reflection (Fig 4) which attributes that magnetite particles of nano iron-oxide has superparamagnetism with magnetization value 0.2774 amu/g which is proportionate to reported value of magnetization particles that make them responsive to magnetic field and possesses enough magnetic response to meet the need of magnetic separation and solid-liquid efficient segregation.

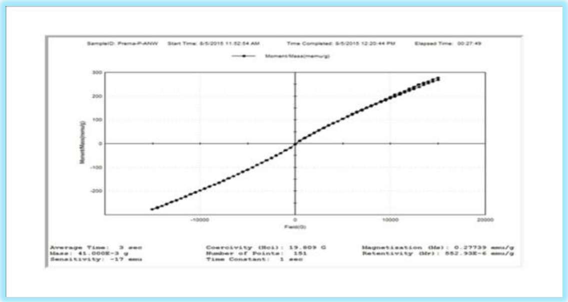

Fig: 4 VSM Curve of PVA-ANM

TEM Analysis:- TEM image (Fig 5) depicted almost cubic iron-oxide particles with an average size of 1-7 nm. The majority of particles were scattered, few of them showing aggregates indicate stabilization of the nanoparticles.

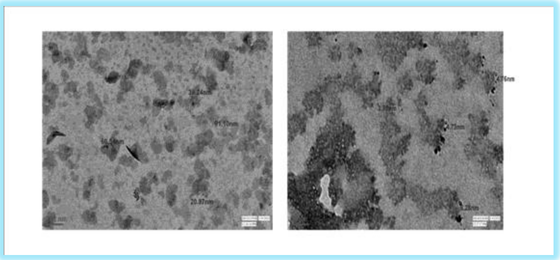

Fig: 5 TEM Image of Nano Iron-Oxide

3.2 Column Parameters of Cd^{+2} uptakes

Effect of Bed Height:- Adsorption breakthrough curves at different bed heights ranging from 2.5 to 10 cm at 1 mL/min flow-rate and 05 mg/L Cd^{+2} ions concentration revealed that throughput volume and column exhaustion time increases with increasing in bed height and adsorption capacity also increases due to availability of more binding site for Cd^{+2} ions uptake by adsorbent (Fig 6) values are given in Table 1.

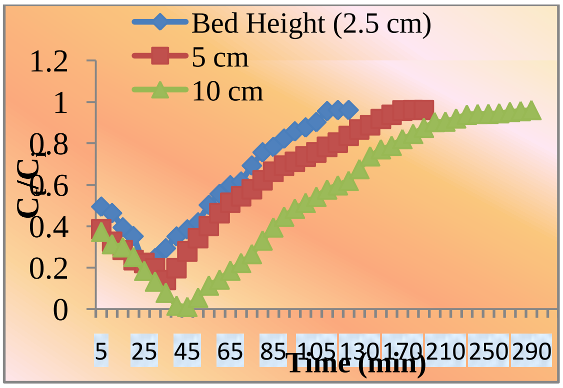

Fig: 8 Breakthrough at various Bed height

Effect of Flow-Rate:- Adsorption breakthrough curves at different flow rates i.e. 1, 2 and 3 mL/min at 05 mg/L Cd+2 ions conc. and 10 cm bed height revealed that column performed well at flow-rate 1 mL/min (Fig 7). By the increase in flow-rate from 1-3 mL/min, breakthrough curves become steeper and reach exhaustion rapidly due to decrease in contact time between adsorbent and adsorbate [31]. Results given in Table-1

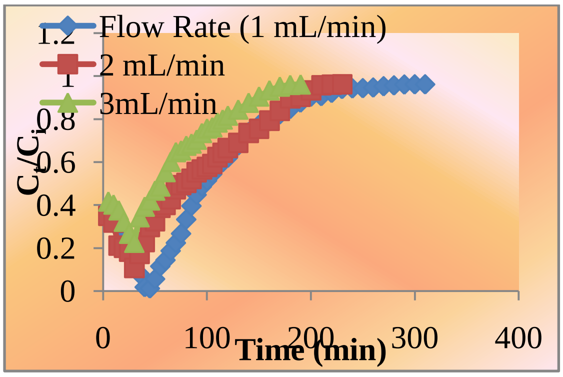

Fig: 7 Breakthrough at different flow- rate

Effect of Cd (II) Ions Concentration:-

Adsorption breakthrough curves at different Cd+2 ions concentrations of 1, 2 and 5 mg/L at flow-rate 1 mL/min and 10 cm bed height Fig 8 revealed that breakthrough time decreases with increasing concentration of Cd+2 ions because binding sites on sorbent surface, saturated more rapidly at higher concentration resulted as early breakthrough time [32], values given in Table 1.

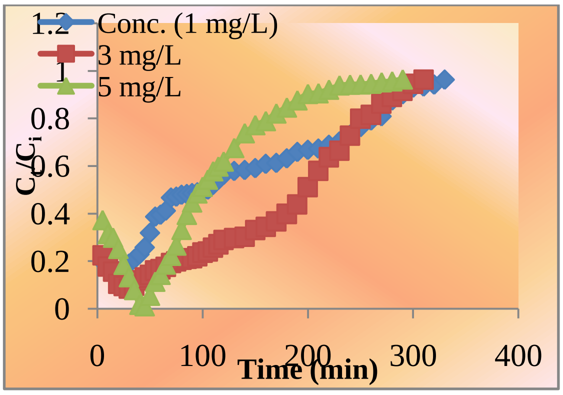

Fig: 8 Breakthrough at various Cd^{+2} Conc.

Table: 1 Results of breakthrough curve at different bed heights, Flow Rates and Cd^{2+} Concentration for Cd^{2+} adsorption onto PVA-ANM microspheres at pH 4, Temp. 25(±2) ℃

S. No.	**Bed Height** cm	**Flow Rate** mL/min	**Cd^{+2} Conc.** mg/L	**t_{total}** min	**q_{total}**	**m_{total}** mg/L	**q_{eq}** mg/g	**% Removal**
1	2.5	1	5	115	0.452	0.575	0.377	78.61
2	5	1	5	180	0.773	0.900	0.594	85.89
3	10	1	5	290	1.433	1.450	0.247	98.83
4	10	2	5	220	1.964	2.20	0.373	89.27
5	10	3	5	170	1.976	2.550	0.432	77.49
6	10	1	1	340	0.288	0.340	0.576	84.71
7	10	1	3	310	0.851	0.930	0.158	91.50

3.3 Modeling Dynamics of Column

Application of Thomas Kinetic Model

Thomas rate constant K_T and maximum uptake Capacity q_o were determine by column data by Eq. 5 and evaluated from slope and intercept of plot $\ln\left(\frac{C_i}{C_t}-1\right)$ vs. V as shown in Fig 9 (a), (b) and (c). The K_T increased with flow rate and reverse trend has shown in bed height and inlet Cd ions concentration. Column sorption capacity q_o increased with increased in concentration and flow-rate of adsorbate but decreased with increased in bed height. Results showed that experimental data well fitted in Thomas model [33, 34] Table 2.

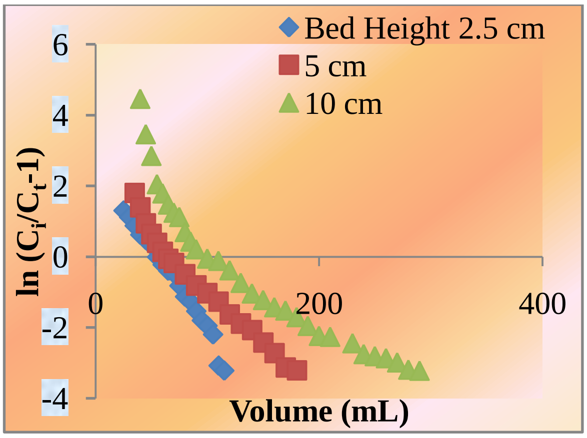

Fig: 9 (a) Thomas Kinetic Model at Various Bed Heights 2.5, 5 and 10 cm

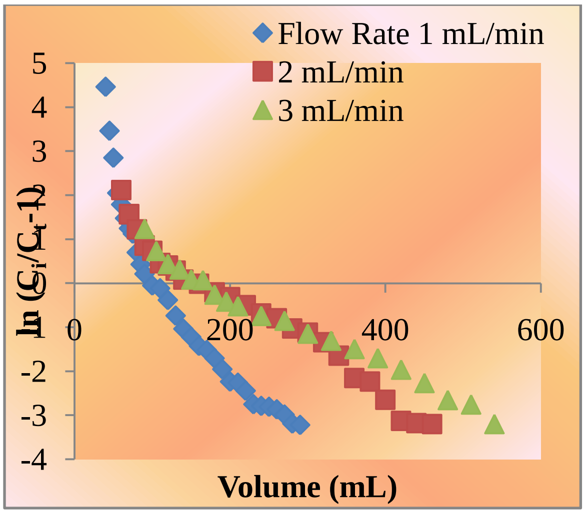

Fig: 9(b) Thomas kinetic model for different flow rate 1, 2 and 3 ml/min

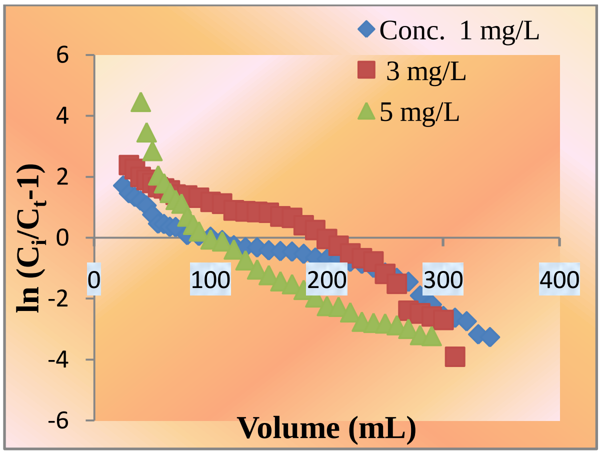

Fig: 9(c) Thomas Kinetic Model for Various Concentrations of Cd^{2+} 1, 3 and 5 mg/L

Table: 2 Thomas Model Parameters of Cd^{2+} Ions Adsorption by PVA-ANM

Factors	Thomas Model Parameters		
	K_T mL/min.mg	q_o mg/g	R^2
Bed Height (cm)			
2.5	4.7	2.635	0.982
5.0	3.1	2.281	0.976
10	2.5	2.895	0.911
Flow Rate (mL/min)			
1	2.5	2.895	0.911
2	1.1	2.05	0.970
3	0.8	1.475	0.980
Cd^{2+} ions Conc. (mg/L)			
1	1.2	1.51	0.934
3	1.7	2.984	0.922
5	2.5	2.895	0.911

Application of Yoon-Nelson Model

Yoon-Nelson model was applied to investigate the breakthrough behavior of column by Eq. 6. KYN and τ were determined from plot between ln $C_t/(C_i$-C_t) vs. t, as shown in Fig 10 (a), (b) and (c). K_{YN} increased with increased in flow-rate and concentration and decreased with increased in bed height, while **τ** increased with bed height but reverse trend obtained in flow-rate and concentration. Y-N model fitted well to experimental parameters. Similar trends obtained in some reported methods [35].

Values are shown in Table 3.

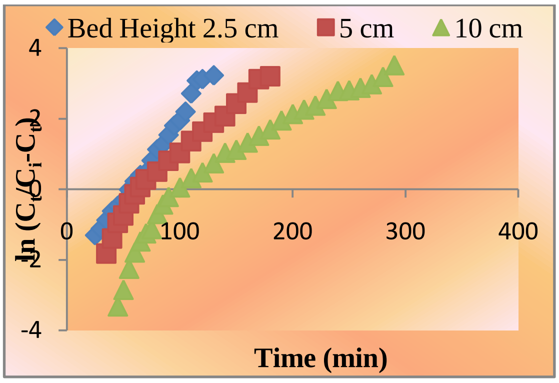

Fig: 10 (a) Yoon-Nelson Kinetic Model at Various Bed Heights 2.5, 5 and 10 cm

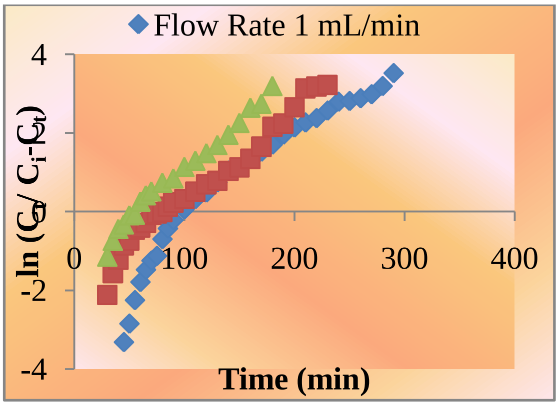

Fig: 10 (b) Yoon-Nelson Kinetic Model at Different Flow Rate 1, 2 and 3 mL/min

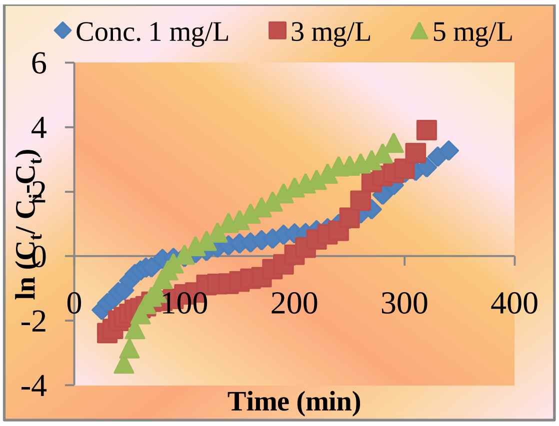

Fig: 10(c) Yoon-Nelson Model at Various Concentration of Cd^{2+} 1, 3 and 5 mg/L

Table: 3 Yoon-Nelson Model Parameters of Cd^{2+} ions adsorption by PVA-ANM

Factors	**Yoon Nelson Model Parameters**			
	K_{YN} min^{-1}	**τ** min	**q_o** mg/g	**R^2**
Bed Height (cm)				
2.5	0.048	57.45	2.662	]0.984
5	0.032	74.36	2.293	0.974
10	0.023	126.15	2.874	0.924
Flow Rate (mL/min)				
1	0.023	126.15	2.874	0.924
2	0.024	83.55	2.016	0.968
3	0.025	57.56	1.458	0.983
Cd^{2+} Conc. (mg/L)				
1	0.012	125.25	1.512	0.938
3	0.018	169.30	3.022	0.932
5	0.023	126.15	2.874	0.924

Application of BDST Model

Bed Depth Service Time model (BDST) stated a relationship between bed height (Z) and service time (t). Kinetic rate constant Ka and bed sorption capacity N_o evaluated by the plot between bed heights vs. time by Eq.7. A straight line with high R^2 value as shown in Fig 11 but is not passing through origin ascribed that the uptake of Cd^{+2} ions from aqueous medium involves more than one rate regulating steps [36]. As the bed height increases the resident duration of liquid inside bed also increases. Results indicated validity of BDST model for present system. Results are given in Table 4.

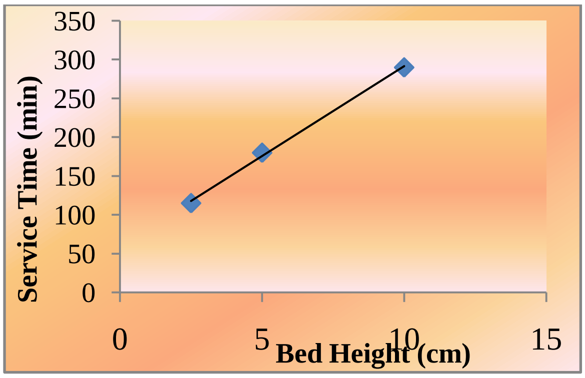

Fig: 11 The BDST Kinetic Model

Table 4: BDST Model Parameters

Cd^{2+} ions Conc. mg/L	**BDST Model Parameters**		
	K_a L/mg. min	**N_o** mg/g	**R^2**
05	0.0149	231.4	0.998

Mechanism of Cd^{+2} ions Adsorption

Binding mechanism of Cd(II) ions onto PVA-ANM takes place in following manner as shown in Fig 13. Cd+2 ions attached through adsorbent by electro-static interaction (a) carboxylic and hydroxyl group of cross-linked alginate, interact with Cd+2 (b) oxy-late group of co-polymeric moiety coordination with Cd+2 (c) electron rich hydroxyl group of polyvinyl alcohol attached with Cd+2 and (d) In addition electron rich oxygen of Fe3O4 nano particles may also co-ordinate with Cd(II) ions.

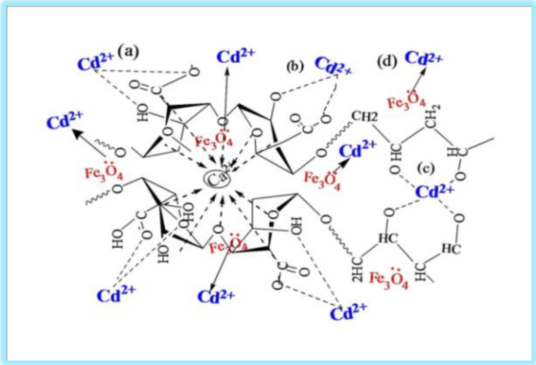

3.4 Column Regeneration

Column with a bed height of 10 cm and feed flow-rate 1 mL/min saturated with 05 mg/L concentration of Cd(II) ions was selected for desorption study. Desorption was carried out by 0.1 M HCl in the down flow manner with 1mL/min flow rate at room temperature. Cd (II) ions concentration was detected after various time intervals. Results of desorption studies are shown in Fig 12 which revealed that >99% recovery of adsorbate in 350 min. Reported nano magnetite adsorbent showed great resilience on sorption capacity after five regeneration cycles. This ascribed that adsorbent could be repeatedly subjected to Cd^{+2} ions treatment without losing its initial uptake efficiency.

Treatment of industrial effluent

The potential of adsorbent tested on sample of industrial effluent containing 02.35 mg/L Cd^{+2} ions by PVA-ANM hydrogel spheres based on experimental results. The adsorbent revealed 97.58% removal of Cd (II) ions.

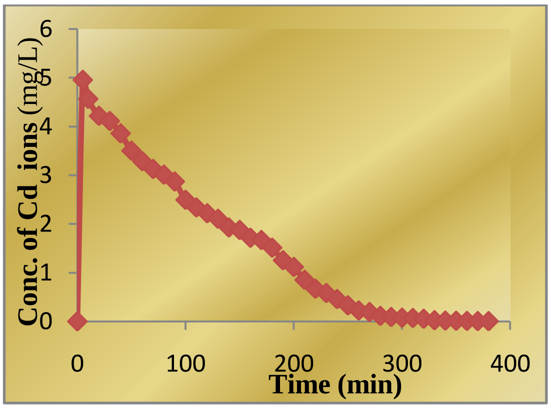

Fig. 12 Desorption of Cd^{+2} Exhausted PVA-ANM Column by 0.1 M HCl

IV. CONCLUSION

Fixed-bed column studies of Cd^{+2} ions adsorption by PVA-ANM were performed with various effects like flow-rate, inlet Cd(II) ions concentration and bed height. Breakthrough curves revealed that equilibrium Cd^{+2} ions adsorption increased with increased in bed height and concentration and decreased with increased in flow-rate. Predicted data fitted well with Thomas, Yoon-Nelson and BDST models. Fixed bed column could be scaled-up for effective sorption by using appropriate parameters of column. Blend mechanics electrostatic interaction with magnetic separation involved in uptake process. Adsorbent demonstrated excellent adsorption capacity (231.4 mg/L) for the removal of Cd(II) ions over a broad range of experimental conditions as well as from effluent sample at room temperature. Reported PVA-ANM hydrogel spheres could be of high potential as low-cost, ecofriendly adsorbent for water remediation. Regeneration with resilience of adsorbent in multiple cycles of usage proved to be a high efficiency adsorbent. Hence it can be used for commercial applications.

ACKNOWLEDGMENTS

The authors are very thankful to UGC-DEA consortium of scientific Research centre for FTIR and XRD & AIIMS New Delhi for TEM analysis.

REFERENCES

[1] Jang S.H., Min B.G., Jeong Y.G., Lyoo W.S. and Lee S.C., J. Hazard. Mater, 152, **(2008)**1285.

[2] Mathialagan T. and Viraraghavan T., Sep. Sci. and Technol., 38, **(2003)** 57.

[3] Jin-ming LUO, Xiao and Sheng-Nonferrous Met. Soc. China, 20, **(2010)**1104.

[4] Low K.S. and Lee C.K., Bioresource Technol., 38(1), **(1991)** 1.

[5] Salim R. Al-Subu M.M. and Sahrhage E., J. Environ. Sci. Health A, 27, **(1992)** 603.

[6] Drush G.A., Sci. Total Environment, 67, **(1993)**75.

[7] Yavuz O., Guzel R., Aydin F., Tegin I., Ziyadanogullari R., Polish J. Environ. Stud. 16, **(2007)** 467.

[8] Saffaj N., Loukil H., Younssi S.A., Albizane A., Bouhria M., Persin M., Larbot A., Desalination, 168, **(2004)** 301.

[9] Qdias H.A., Moussa H., Desalination, 164, **(2004)** 105.

[10] Alvarez-Ayuso E., A. Garcia-Sanchez, X. Querol, Water Res. 37**, (2003)** 4855.

[11] Chen G.H., Sep. Purification Technol. 38, **(2004)** 11.

[12] Crini G., Bioresource Technology, 97, **(2006)** 1061.

[13] Choksi P.M., Joshi V.Y., Desalination, 208, **(2007)** 216.

[14] Gerente C., Lee V.K.C., Le Cloirec P., Environ. Sci. Technol. 37, **(2007)** 41.

[15] Xiao X., Luo S., Zeng G., Wei W., Wan Y., Chen L., Yang L., Chen J. and Xi Q., Bioresource Technol., 101(6), **(2010)** 1668.

[16] Hidalgo-Vázquez A.R., Alfaro-Cuevas-Villanueva R., Márquez-Benavides L. and Cortés-Martínez R., J. of Appl. Sci. in Environ. Sanitation, 6 (4), **(2011)** 447.

[17] Orhan Y. and Buyukgungor H., Water Science and Technology, 28, **(1993)** 247.

[18] Brown P., Jefcoat I. A., Gill S. and Graham, E., Adv. in Environ. Research, 4, **(2000)** 19.

[19] Singh K. K., Talat M. and Hasan S. H. Bioresource Technol., 97 **(2006)** 2124.

[20] Taty-Costodes V.C., Fauduet H., Porte C. and Delacroix A., J. of Hazard. Mater. B, 105 **(2003)** 121.

[21] Kumar U. and Bandyopadhyay M., Bioresource Technol., 97 **(2006)** 104.

[22] Ghimire K. N. Inoue J. I., Inoue K., Kawakita H. Ohto K., Sep. Sci. and Technol., 43 **(2008)** 362.

[23] Blázquez G., Hernainz I., Calera M. and Ruiz-Núñez L.F. Process Biochem., 40 **(2005)** 2649.

[24] Tangjuank S., Insuk N., Tontrakoon J. and Udeye V., World Academy of Sci., Engg. and Technol., 52, **(2009)**110.

[25] Namasivayam C. and Ranganathan K., Water Res, 29 (7), **(1995)** 1737.

[26] Dhiwar C., Tiwari A. and Bajpai A.K., J. of Dispersion Sci. and Technol., 32, **(2011)**1661.

[27] Dewangan T., Tiwari A. and Bajpai A.K., J. of Dispersion Sci. and Technol., 32, **(2011)**1075.

[28] Essawy H. A., Ibrahim H.S., React. Funct. Polym., 61 **(2004)** 421.

[29] Sharma N. and Tiwari A., Research J. of Chem. Sci., 4 (9) **(2014)** 88.

[30] Gupta A.K., Wells S., IEEE Transactions on Nano bioscience, 3, **(2004)** 66.

[31] Sarin V., Singh T.S. and Pant K.K., Bioresource Technol., 97, **(2006)** 1986.

[32] Vijavaraghavan K., Jegan J., Palanivelu K., Velan M., Chem. Eng. J., 106, **(2005)** 177

[33] Chowdhury Z.Z., Zain S.M., Khan R.A., Rafique R.F. and Khalid K., Bioresource Technol., 7(3), **(2012)** 2895.

[34] Baral S.S., Das N., Ramulu T.S., Sahoo S.K., J. Hazard. Mater., 161, **(2009)** 1427.

[35] Ahmad A.A. and Hameed B.H., J. Hazard. Mater., 175, **(2010)** 298

[36] Ko D.C.K., Porter J.F. and Mckay G., Chem. Eng. Sci., 5, **(2000)** 5819.

◆◆◆